Supplemental Figure Legends

Supplemental Figure 1: Characterization of Inhibitor Effects on Human CD34+ HSPC-induced Erythroid Differentiation. (A) LSD1 inhibition by a novel, reversible LSD1 inhibitor, CCG50 (LSDi). (B) Schematic summarizing the timing and duration of media supplements (hydrocortisone, IL3, SCF and EPO) to *in vitro* erythroid differentiation of human CD34+ HSPCs. Hydrocortisone and human IL-3 were withdrawn on day 7 when the LSD1 inhibitor(s) were added; human SCF was withdrawn from the culture medium on day 11. (C) Representative flow cytometric cell count of CD34+ HSPCs after 7 days of induced erythroid differentiation (prior to LSD1 inhibitor treatment) analyzed using anti-CD71 and anti-CD235a erythroid antibodies.

Supplemental Figure 2: Mouse *Gata1* BAC recombination strategy. A creER^{T2}-PolyA-Neo cassette[25,31] was targeted to the ATG start codon in exon 2 of a 196 kb wild type mouse *Gata1* BAC (*G1B*). Subsequently, the Neo selection cassette was removed from the recombinant *G1B*CreER^{T2}-Neo BAC to generate the final *G1B*CreER^{T2} BAC, which was used to generate transgenic mice.

Supplemental Figure 3: *G1B*CreERT2 is not active in non-erythroid hematopoietic lineages. Tandem tomato (TdT) epifluorescence was not detectable in BM cells stained with B220+, Gr1+, CD11b+ or CD3ε+ antibodies in either *G1B*CreER^{T2} lines L245 or L259 treated with Tamoxifen (red peak). R26T:*G1B*CreER^{T2} mice that were not treated with Tx served as negative controls (blue peak).

Supplemental Figure 4: *G1B*CreER^{T2} is expressed in a minor fraction of megakaryocytes and mast cells. Representative flow cytometric diagrams depicting the gating cutoffs for megakaryocytic progenitor cells (MkPs; Lin-cKit+Sca1-CD41+CD150+; A, B), megakaryocytes (Mk; CD61+CD41+; C, D) or mast cells (FceRIa+c-Kit+; E, F) in the BM of untreated (left panels in A, C and E; blue peaks in B, D and F) or Tx-treated (right panels in A, C and E; red peaks in B, D and F) R26T:*G1B*CreER^{T2} L259 mice. Representative flow histograms depict TdT (red peaks) in very few MkPs (B), but in more Mk (D) and mast cells (F).

Supplemental Figure 5: Gating strategies for CFU-E and megakaryocytic progenitor cell populations. Total BM cells from untreated (left panels) or Tx-treated (right panels) R26T:*G1B*CreER^{T2} L259 mice were stained with the indicated lineage antibodies. Representative flow diagrams depicting the gates used to identify CFU-E (Lin-cKit+Sca1-CD41-CD16/32-CD150-CD105+) and megakaryocytic progenitors **(**MkPs; Lin-cKit+Sca1-CD41+CD150+), which were analyzed for TdT epifluorescence in Fig.s 2C and S4, respectively.

Supplemental Figure 6: Gating strategies for LSK, CMP, GMP and MEP populations. Total BM cells from untreated (left panels) or Tx-treated (right panels) R26T:*G1B*CreER^{T2} L259 mice were stained with Lineage, c-Kit, Sca1, CD34 or CD16/32 antibodies. Representative flow plots and labels depict the gates used for LSK **(**Lin-c-Kit+Sca1+), CMP **(**Lin-c-Kit+Sca1-CD16/32-CD34+), GMP (Lin-c-Kit+Sca1-CD16/32+CD34+) and MEP (Lin-c-Kit+Sca1-CD16/32-CD34-) populations, which were further analyzed for TdT epifluorescence in Fig. 2C.

Supplemental Figure 7: Gating strategies for CMP, GMP and MEP populations. The CD41-CD16/32- LK fraction was separated by CD105 and CD150 for CFU-E staining as shown in Figure 3. The LK fraction was separated by CD34 and CD16/32 for CMP, GMP and MEP staining in Figure 4.

Supplemental Figure 8: CFU-E cell death is comparable in *Lsd1*-CKO and control mice. The cell death of CFU-E cells in Figure 3D was analyzed by AnnexinV staining.

Supplemental Figure 9: Erythroid precursor cells in *Lsd1*-CKO mice exhibit reduced cell death. The apoptotic cell death of BasoE, PolyE and OrthoE in Fig. 3F was assessed by AnnexinV staining. Data are shown as the means ± SD. (** p<0.01; unpaired Student's t-test).

Supplemental Figure 10: The cell cycle status of erythroid precursors in *Lsd1*-CKO and control mice is statistically unchanged. The distribution of CD71+Ter119+ cells depicted in Figure 3F was analyzed by DAPI staining. Data is shown as the mean ± SD. (**

p<0.01; unpaired Student's t-test). 2N, cells in G1 phase; S, cells in S phase; 4N, cells in G2/M phase of the cell cycle.

Supplemental Figure 11: GMP in *Lsd1*-CKO mice exhibit significantly diminished cell death. Cell death in phenotypic GMP (shown in Fig. 4A) was analyzed by AnnexinV staining. Data are shown as the means ± SD. (** *p*<0.01; unpaired Student's t-test).

Supplemental Figure 12: LSD1 directly inhibits myeloid differentiation genes in erythroid cells. (A) Histograms depicting the relative mRNA levels of human PU.1, CEBPα, RUNX1 and GATA1 (normalized to OAZ1 transcript level[15]) in human CD34+ cells after 14 days of erythroid differentiation as assayed by qRT-PCR. Cells were expanded in the presence of DMSO or LSD1 inhibitors TCP (3 μM) or LSD1i at three different concentrations. (B) ChIP-qPCR analysis of LSD1 binding to the *PU.1* promoter in HUDEP2 cells. Differential enrichment was detected at the *PU.1* transcriptional start site (TSS, black bar), but not at an adjacent site (TSS +27kb) included as a negative control (gray bar). Rabbit IgG was included as a negative antibody control. Data are shown as the means ± SD. (* *p*<0.05; ** *p*<0.01; *** *p*<0.001; unpaired Student's t-test).

Supplemental Figure 13: Sanger sequencing data of *PU.1* -/- HUDEP2 clones. Individual HUDEP2 clones were subjected to genomic DNA extraction, the genomic DNA locus of sgRNA cutting sites were amplified by PCR, the amplicons were subcloned into a sequencing vector and the sanger chromatogram showing data surrounding the guide cutting sites are shown. Note, clone P2-25 has two PCR products of different sizes; clone P3-14 and P3-18 have only one PCR product; while clone P2-4 has no PCR product.

Supplemental Figure 14: Sanger sequencing data of *RUNX1* -/- clones. Individual clones were subjected to genomic DNA extraction, the genomic DNA bearing sgRNA cutting sites was amplified by PCR, the amplicons were subcloned into sequencing vectors and the sanger chromatogram data surrounding the cutting sites is shown.

Supplemental Figure 15. *PU.1* or *RUNX1* genetic loss rescues HUDEP2 cells from the differentiation inhibition caused by LSD1 inhibitor treatment. CD71/CD235a flow

cytometric analysis of three different non-specific sgRNA-infected cells (NT1, NT3 and NT4, left), four *PU.1*-/- clones (middle panels) or four *RUNX1*-/- clones (right panels) treated with **(A)** DMSO or **(B)** 300 nM CCG50 LSD1i for four days after the induction of erythroid differentiation.

Supplemental Figure 16. RUNX1 inhibitor co-treatment partially rescues the differentiation toxicity of LSD1 inhibitor CCG50. (A) Human CD34+ HSPC were expanded for 7 days; on day7, cells were reseeded and treated with LSD1 inhibitor CCG50 or RUNX1 inhibitors (Ro5 or A-10-104) or both inhibitors. **(B)** CD71/CD235a staining of differentiating human CD34+ cells at day 9, 2 days after the addition of CCG50, RUNX1 inhibitor Ro5-3335, RUNX1 inhibitor AI-10-104 (A104) or both LSD1 and RUNX1 inhibitors.

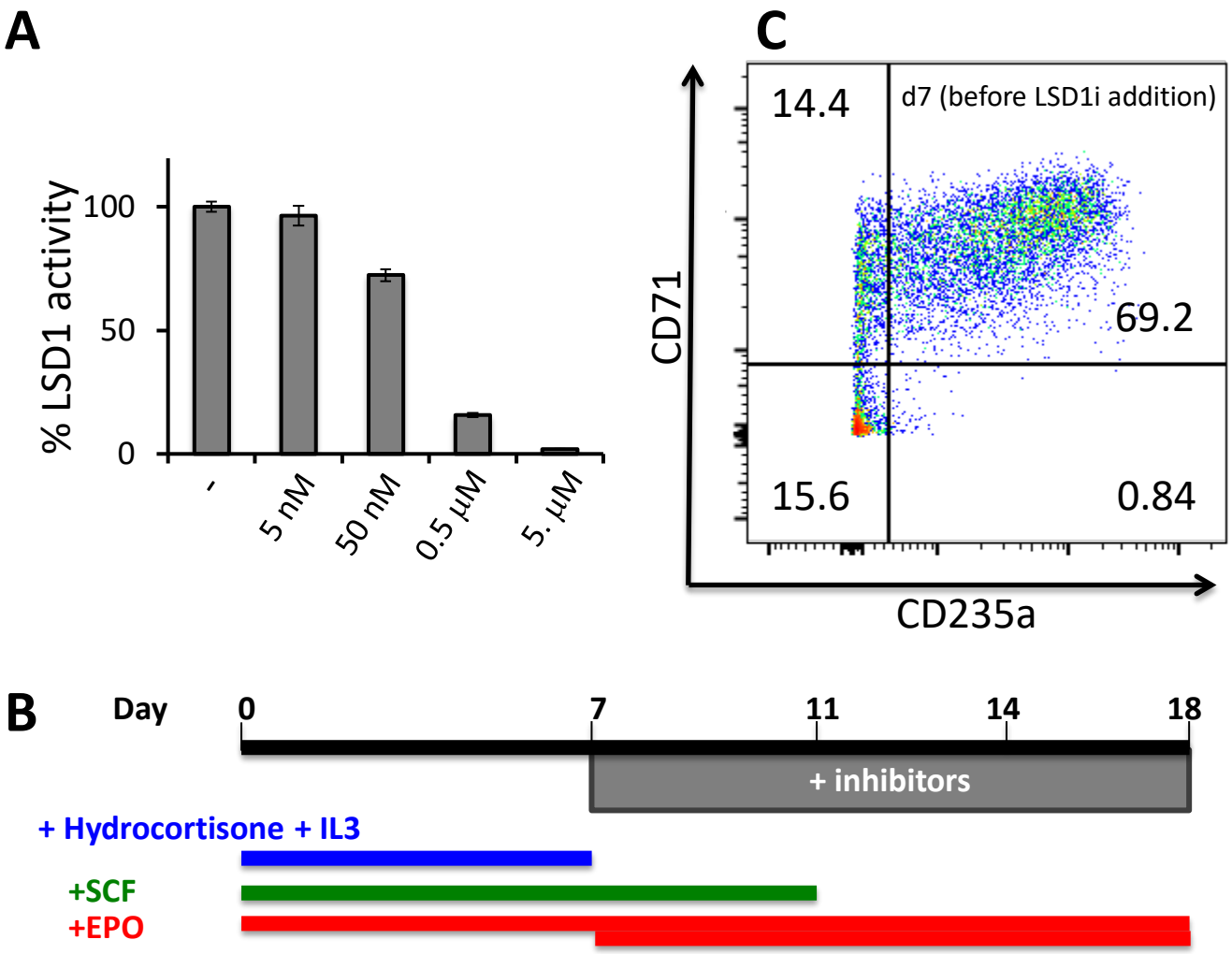

Flow Cytometry	D7	D11	D14	D18
RNA collection			D14	
HPLC Analysis				D18

Supplemental Figure 1.

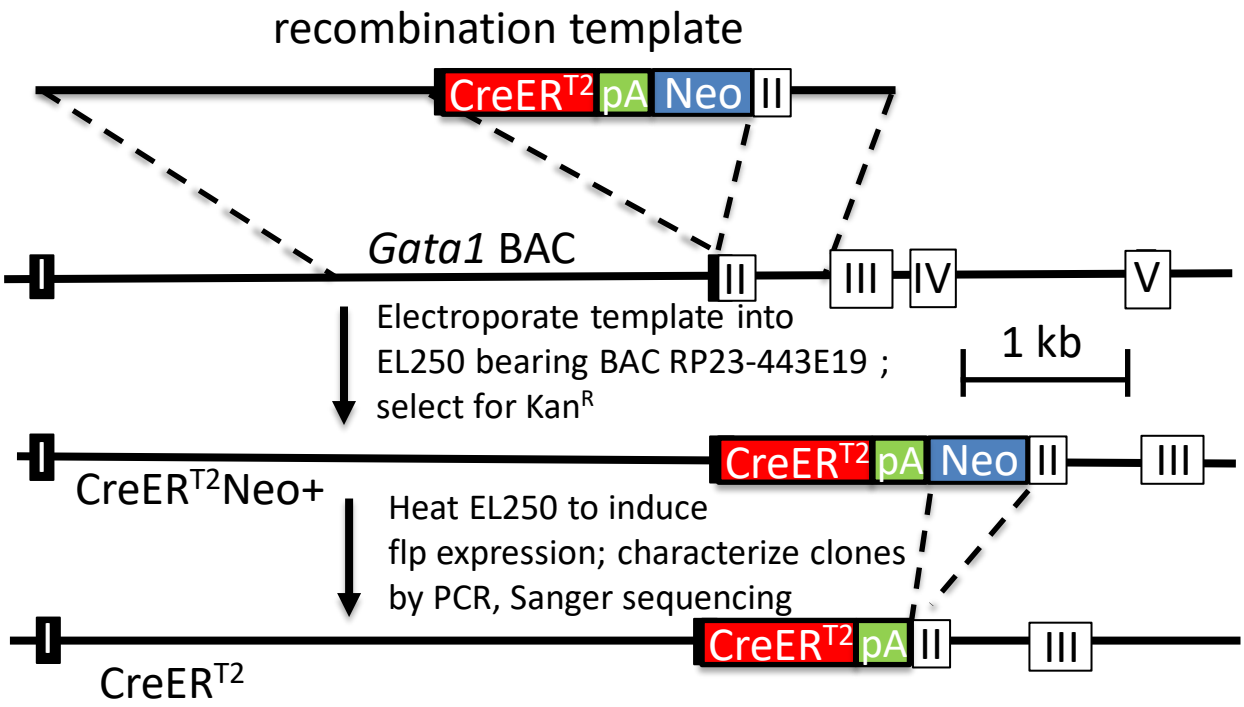

Supplemental Figure 2.

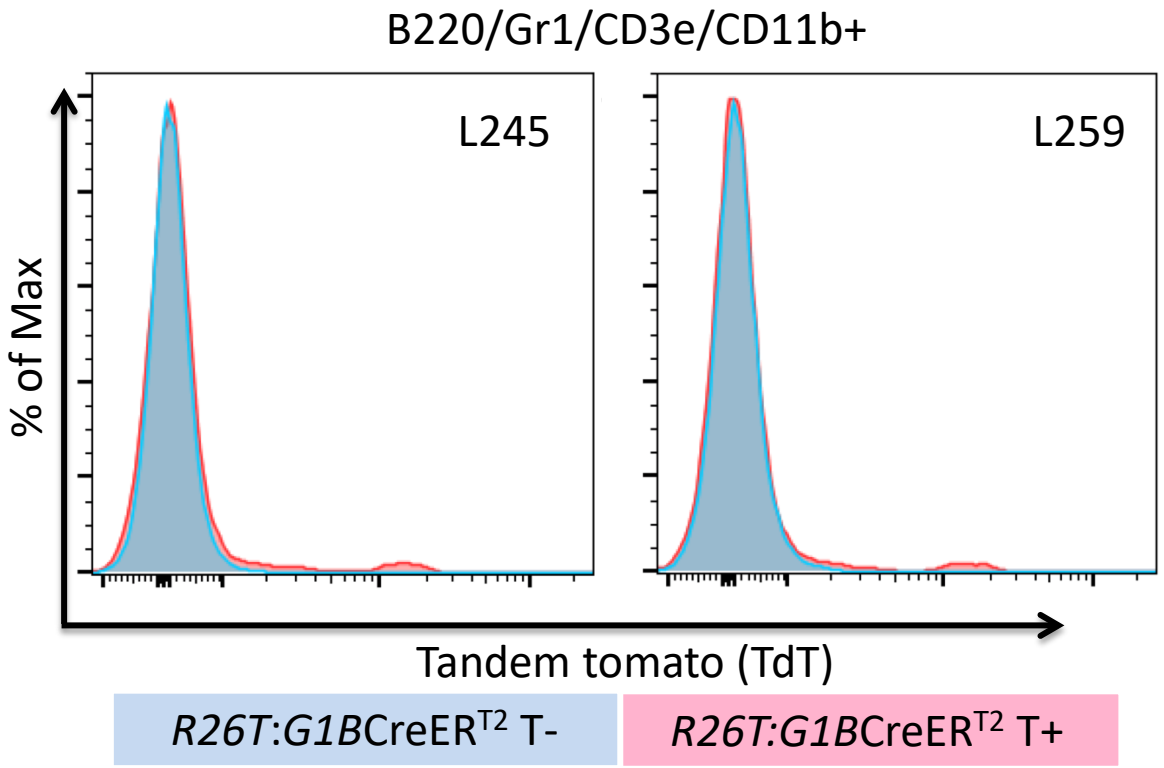

Supplemental Figure 3.

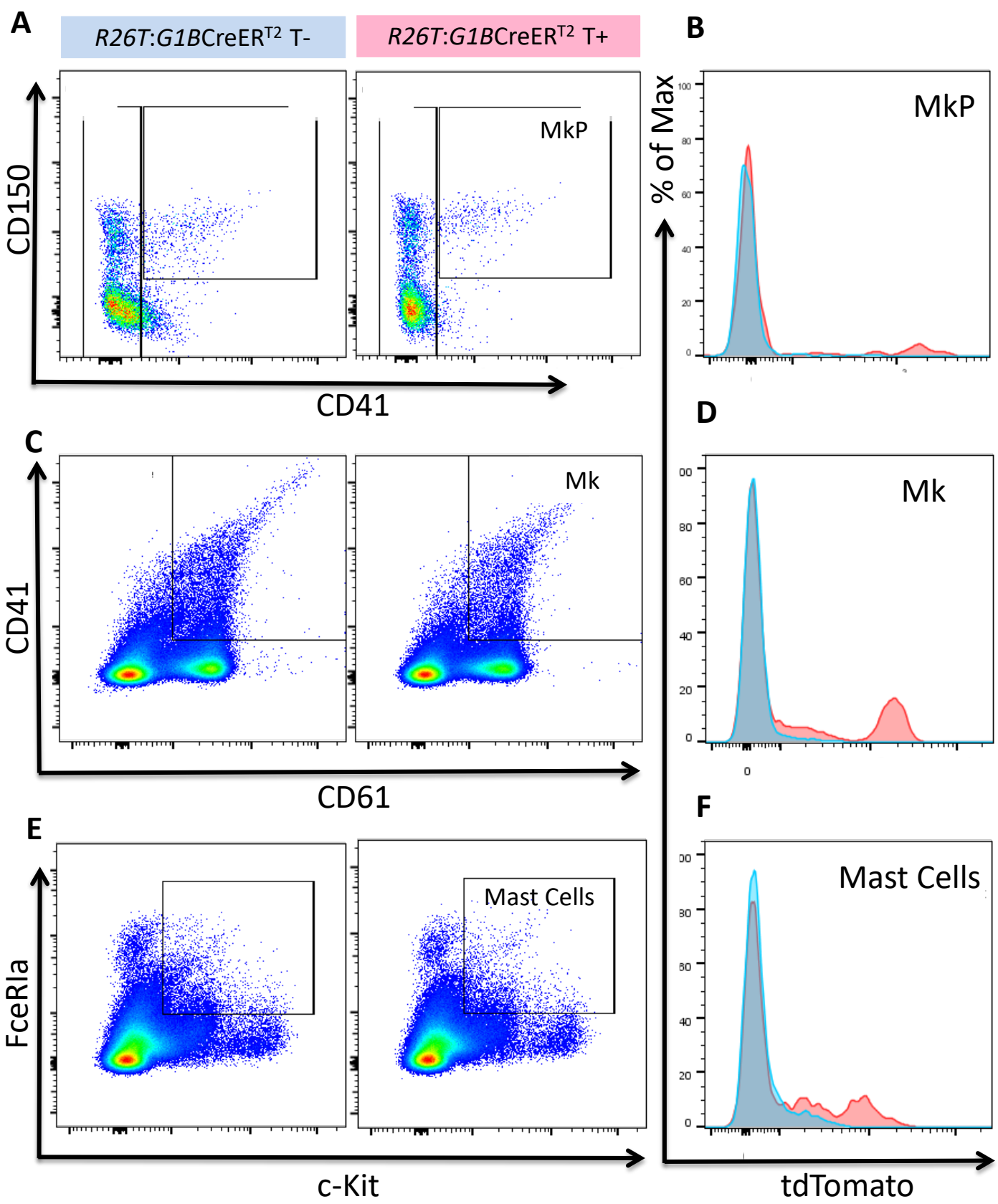

Supplemental Figure 4.

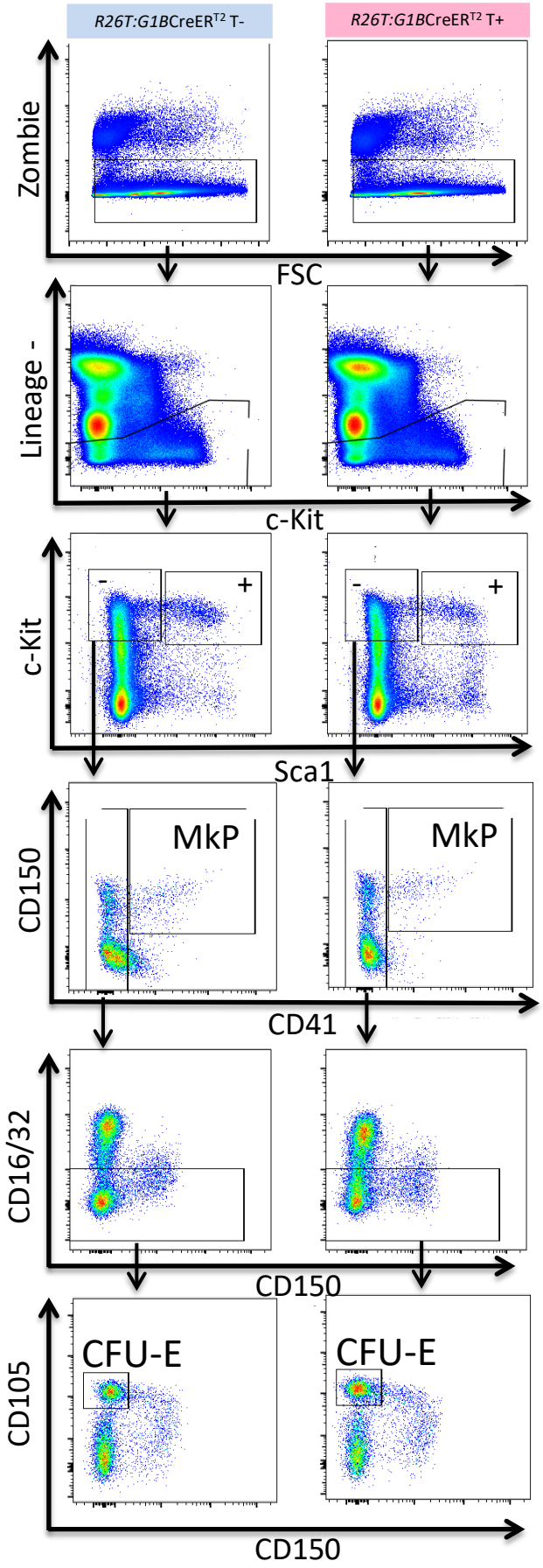

Supplemental Figure 5.

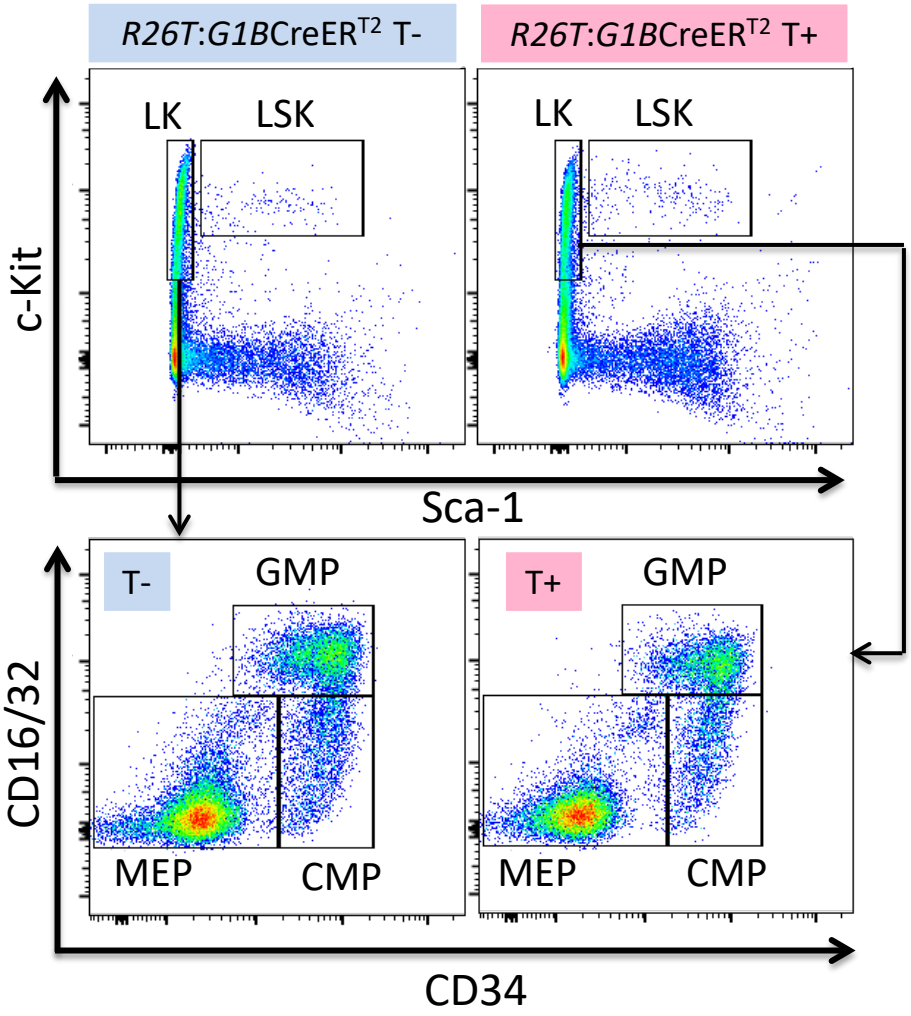

Supplemental Figure 6.

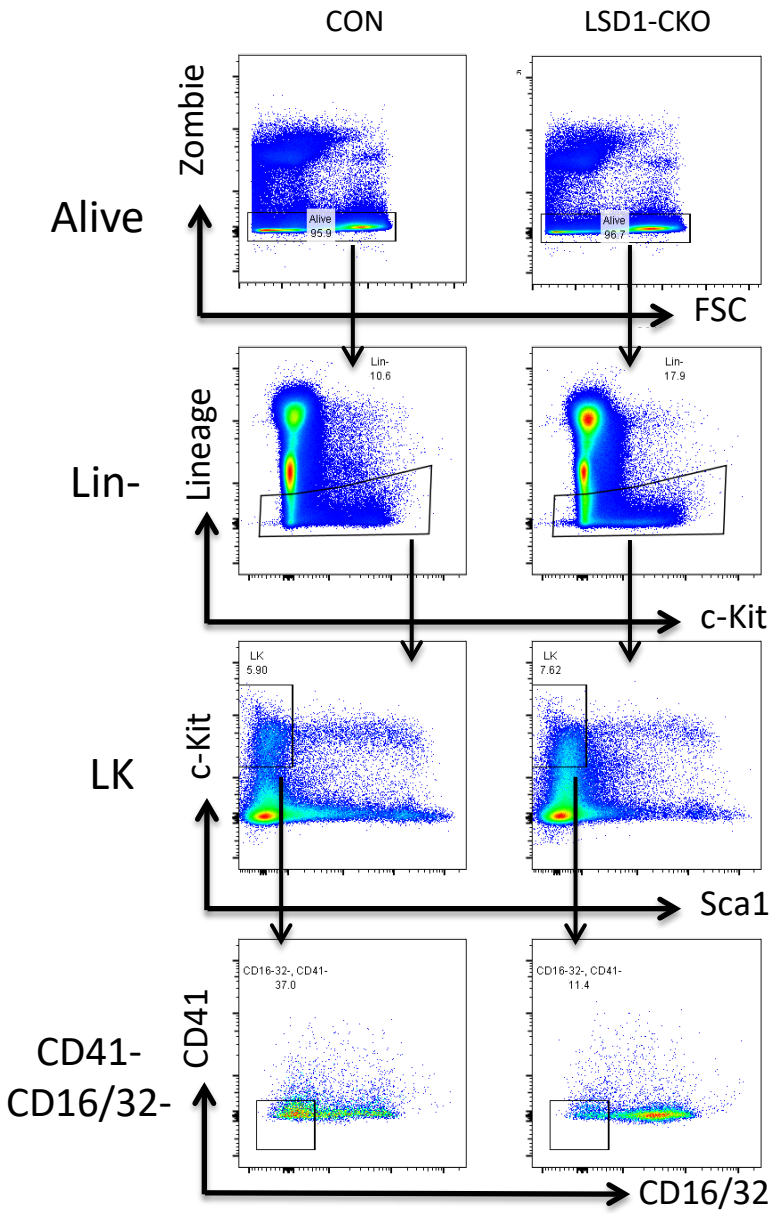

Supplemental Figure 7.

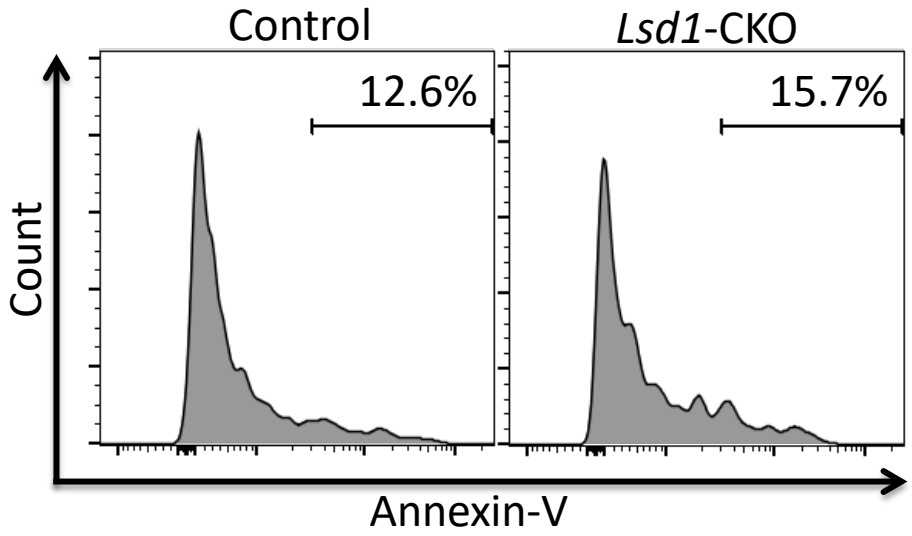

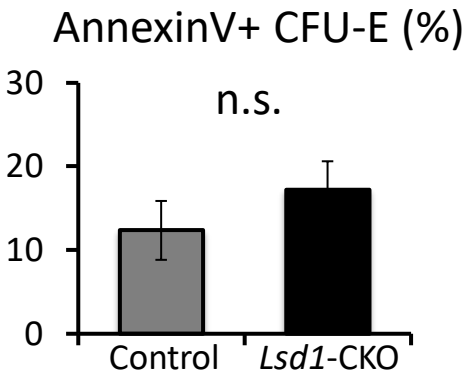

Supplemental Figure 8.

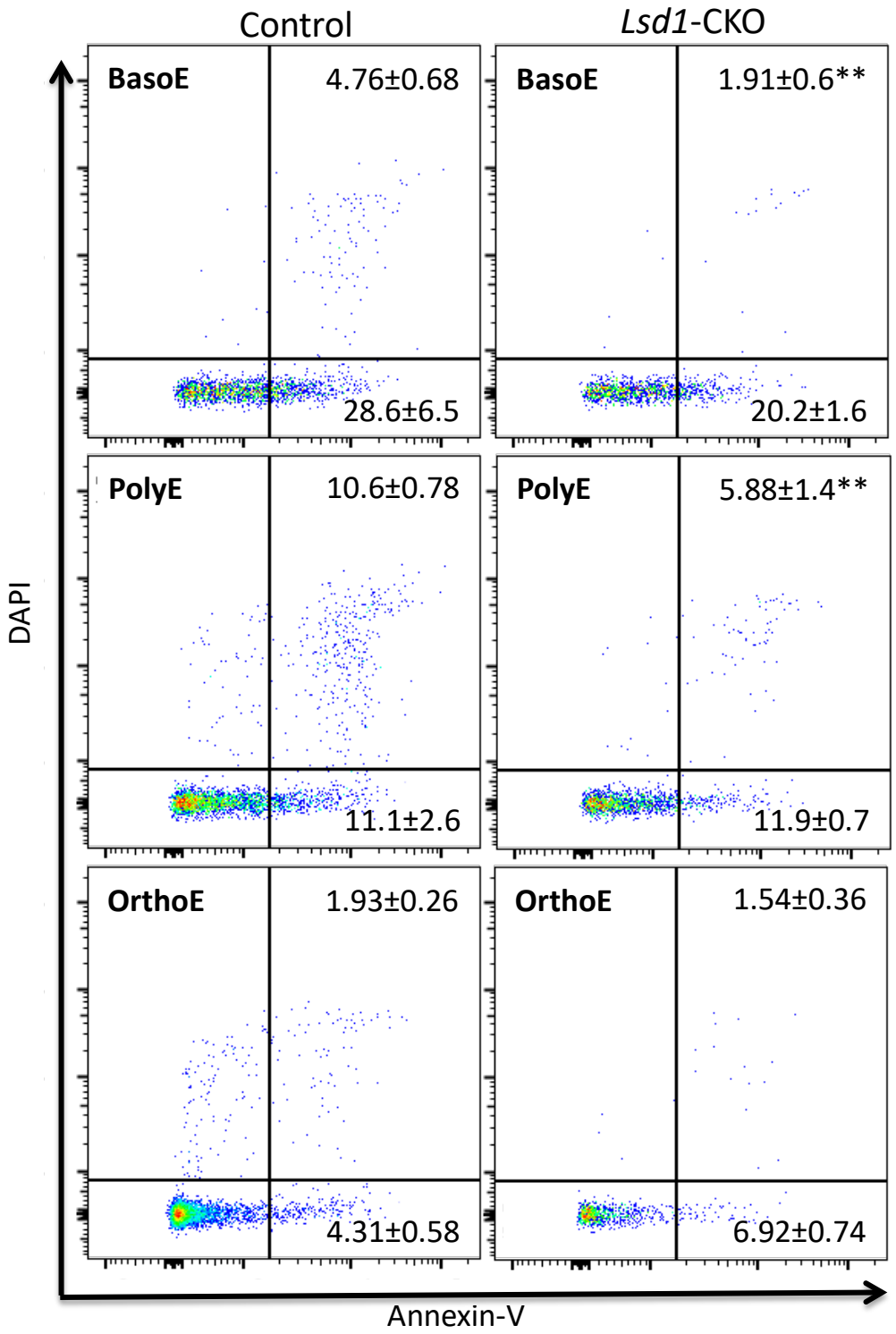

Supplemental Figure 9.

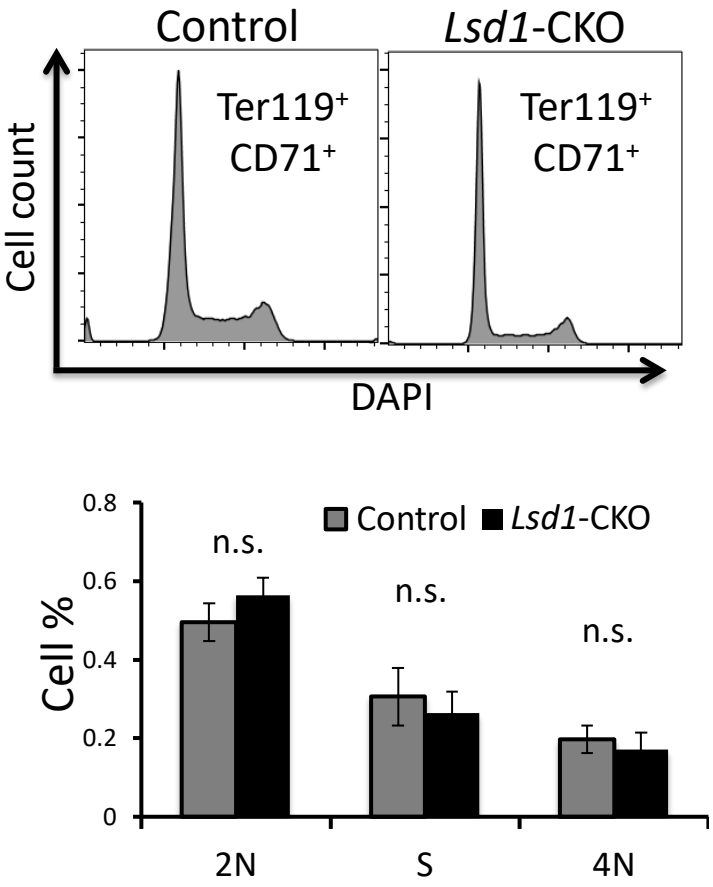

Supplemental Figure 10.

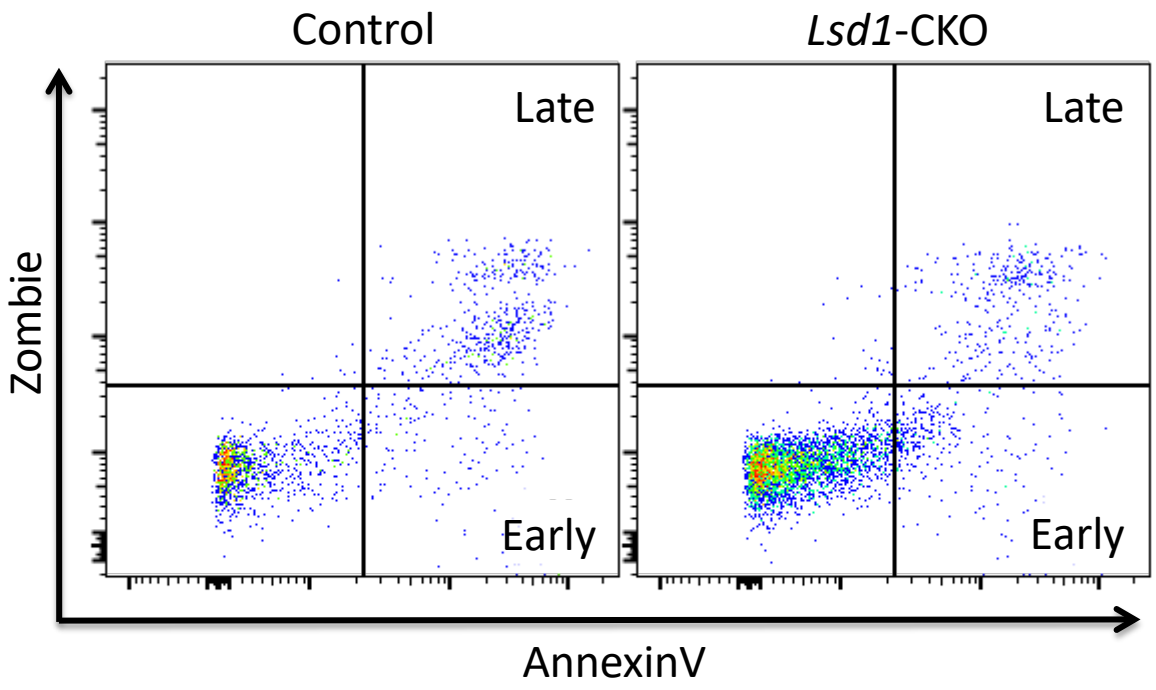

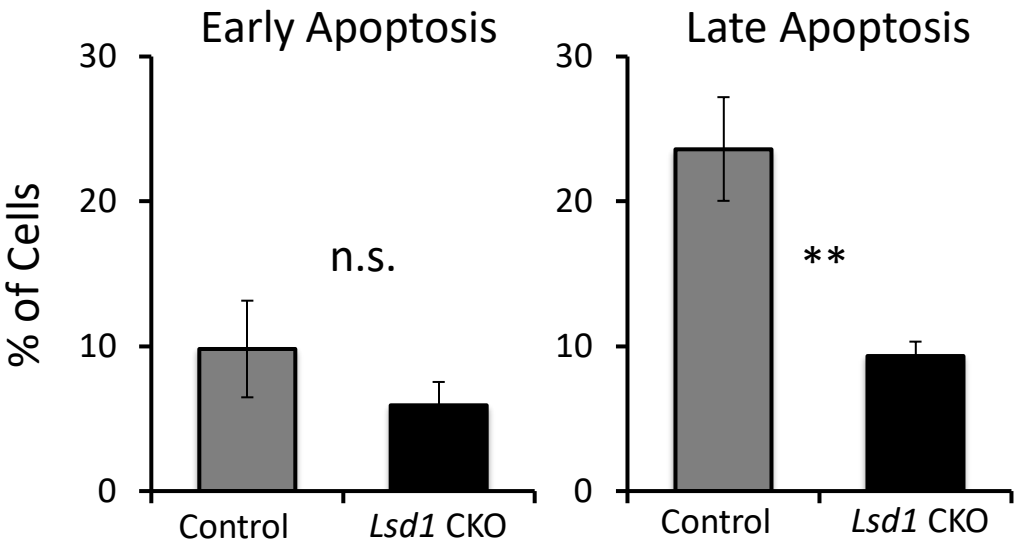

Supplemental Figure 11.

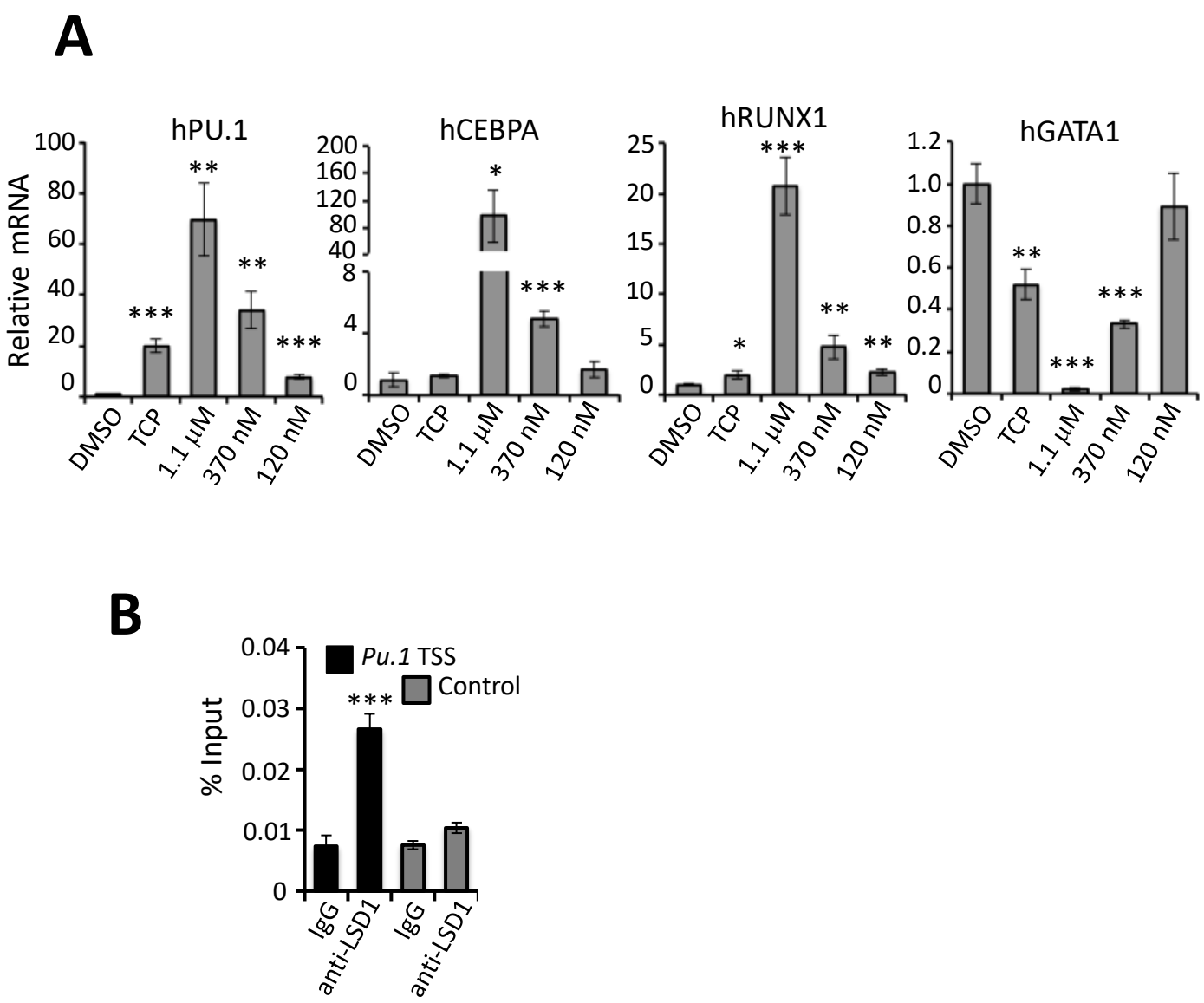

Supplemental Figure 12.

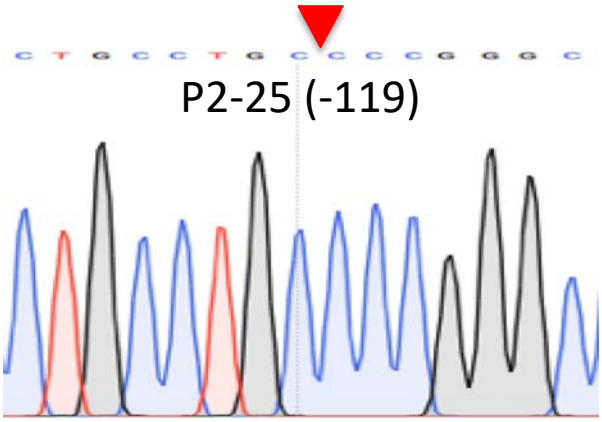

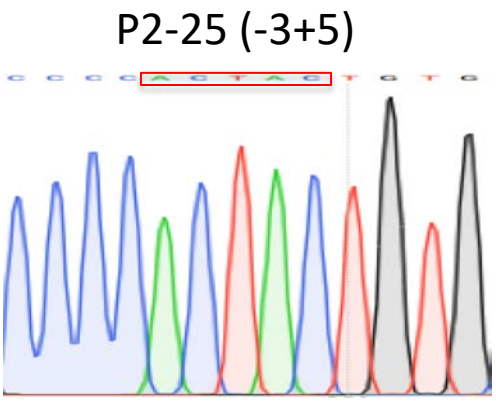

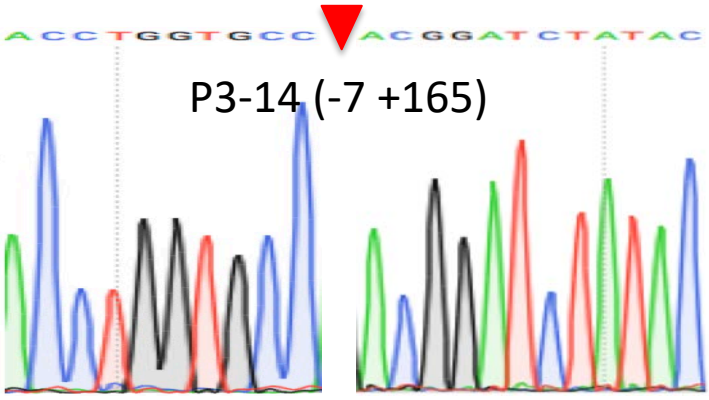

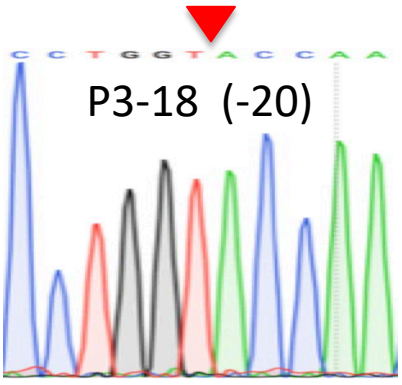

Supplemental Figure 13.

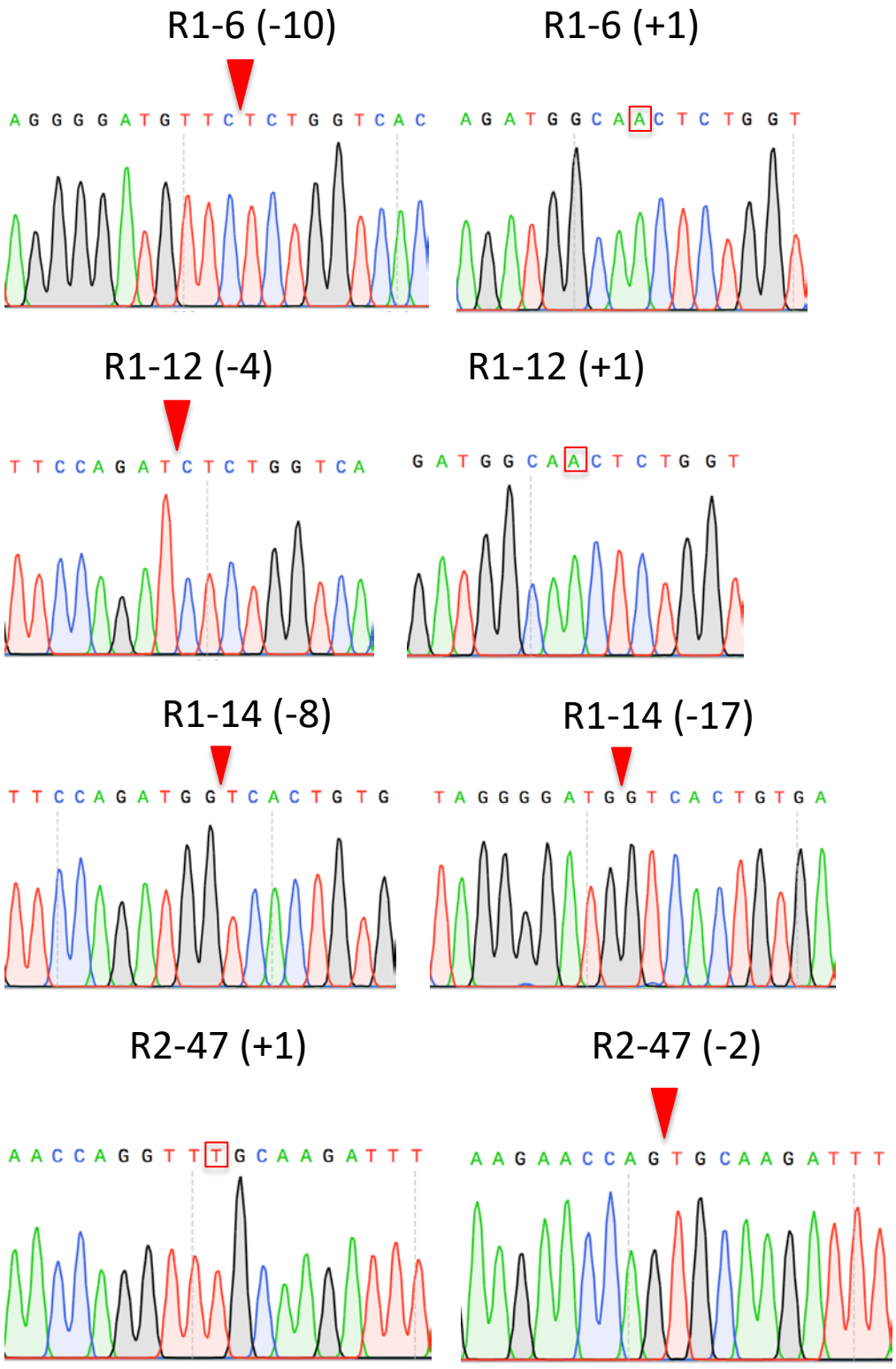

Supplemental Figure 14.

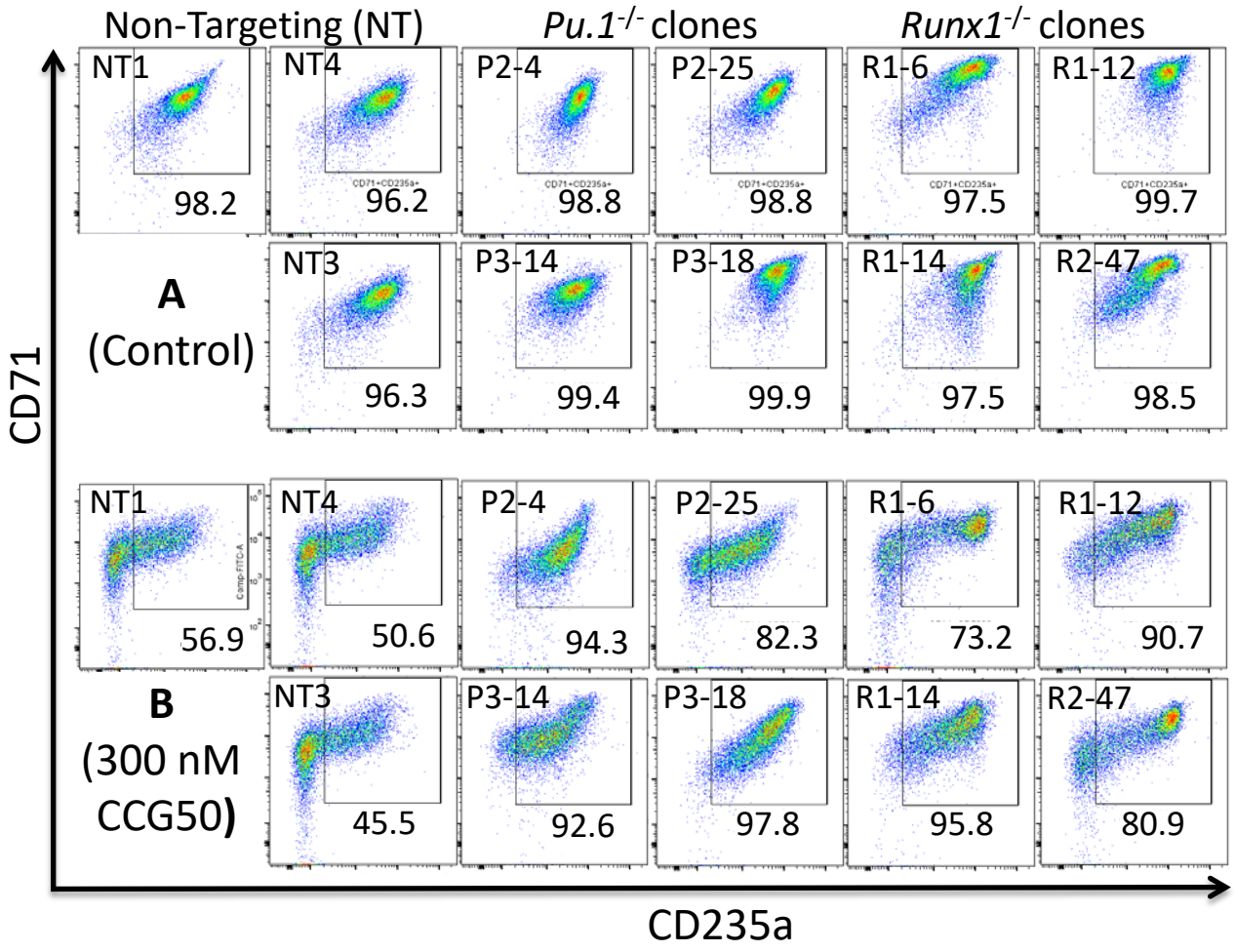

Supplemental Figure 15.

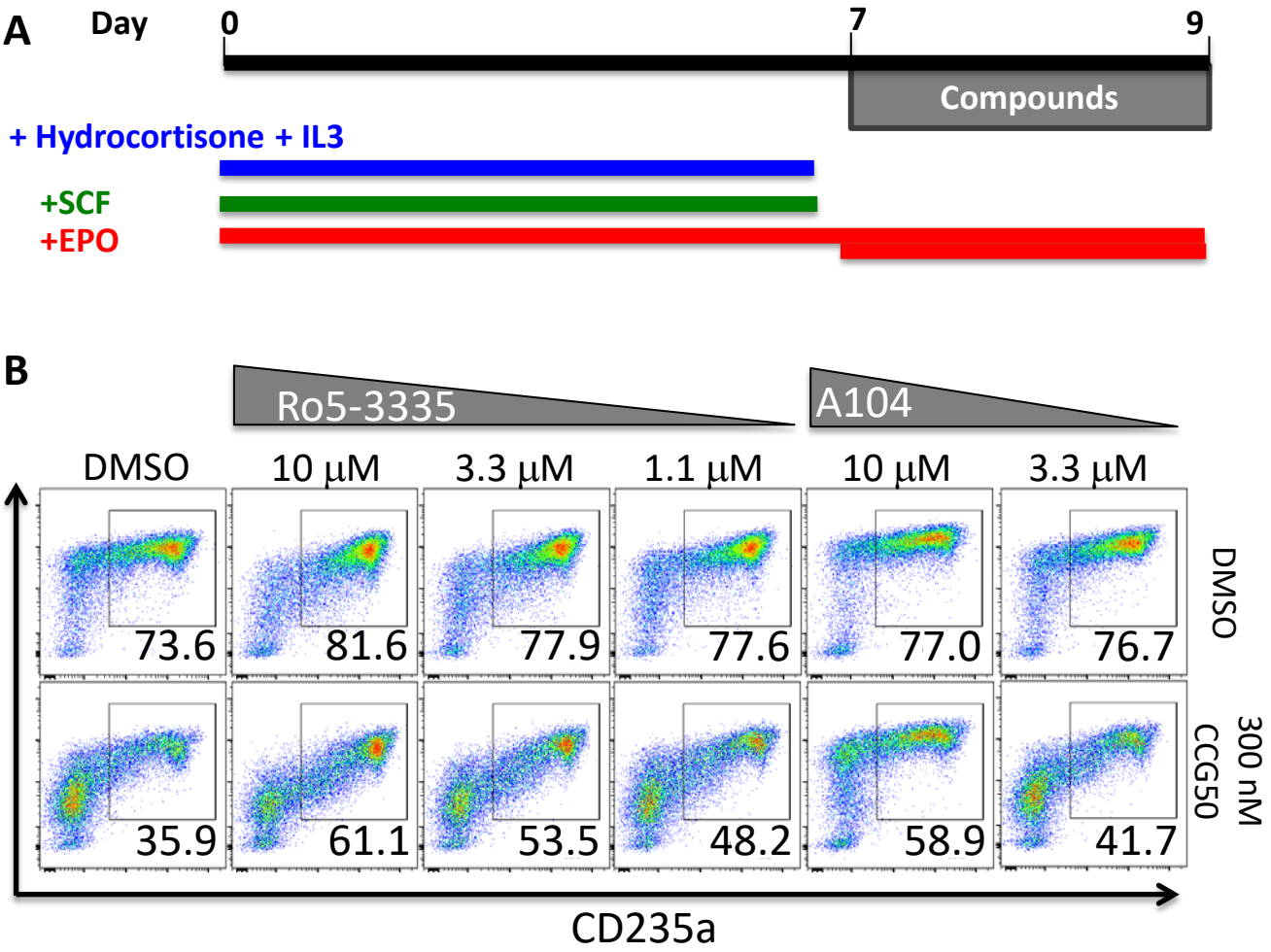

Supplemental Figure 16.

Supplemental Table 1. Sequences of all DNA oligonucleotides used in these studies,

Mouse Genotyping	**Forward 5' to 3'**	**Reverse 5' to 3'**
Lsd1 flox	AGCTACAGCACCAACACTAAAGAG	CAGCAGCTCGACAGCTACAGAGTT
CAT	CAGTCAGTTGCTCAATGTACC	ACTGGTGAAACTCACCCA
Cre	ACGTTCACCGGCATCAACGT	CTGCATTACCGGTCGATGCA
ERT2	GACAGGGAGCTGGTTCACAT	AGAGACTTCAGGGTGCTGGA
R26T	CTGTTCCTGTACGGCATGG	GGCATTAAAGCAGCGTATCC
Real time qPCR	**Forward 5' to 3'**	**Reverse 5' to 3'**
Human OAZ1	GACAGCTTTGCAGTTCTCCTGG	TTCGGAGCAAGGCGGCTC
Human γ-globin	TGGATCCTGAGAACTTCAAGC	CACTGGCCACTCCAGTCAC
Human β-globin	AGGAGAAGTCTGCCGTTACTG	CCGAGCACTTTCTTGCCATGA
Human GATA1	CACTGAGCTTGCCACATCC	ATGGAGCCTCTGGGGATTA
Human KLF1	GGGAGCCTCTTACGGAAAAT	TGCACGACAGTTTGGACATC
Human TAL1	GTACCCCCGTAGCGGAAA	AGGTGTCTACGCGGTTGC
Human PU.1	GACACGGATCTATACCAACGCC	CCGTGAAGTTGTTCTCGGCGAA
Human RUNX1	CCACCTACCACAGAGCCATCAA	TTCACTGAGCCGCTCGGAAAAG
Human CEBPA	GCAAATCGTGCCTTGTCAT	CTCATGGGGGTCTGCTGTAG
Mouse RUNX1	CACCGTCTTTACAAATCCGCCAC	CGCTCGGAAAAGGACAAACTCC
Mouse PU.1	GAGGTGTCTGATGGAGAAGCTG	ACCCACCAGATGCTGTCCTTCA
Mouse LSD1	CGATACTGTGCTTGTCCACCGA	CCAAGCCAGAAACACCTGAACC
Mouse GATA1	ACGACCACTACAACACTCTGGC	TTGCGGTTCCTCGTCTGGATTC
Mouse 18S rRNA	CTCAACACGGGAAACCTCAC	CGCTCCACCAACTAAGAACG
Lsd1 deletion P1	TCAGGTGTTTCTGGCTTGG	CTCTTACCCTGGCTTCCAGA
Lsd1 deletion P2	TAGTTAGGCAGGCAGCAGGT	GCAGCAGACATTGCTCAAAC
ChIP assay	**Forward 5' to 3'**	**Reverse 5' to 3'**
huPu.1 TSS	TCTCTTGCGCTACATACAGGAA	ATCCCTCTCAGTCCCAGCTT
huPu.1 -14kb	AATGGGCTGTTGGCGTTTTG	CTGAGAAAACAGGAAGCGCC
huPu.1 +27kb	AAACCTCAGGGAAGGCTGAT	ACCAGGGATCTTACGCAGTC
***Gata1* BAC recombination**	**Forward 5' to 3'**	**Reverse 5' to 3'**
5' Homologous region	ATCGGAATTCCGCGGAA GTTGGGGAGCACAGAAG	ATCGGAATTCGGGAACACT GGGGTTGAA
3' Homologous region	ATCGGAATTCTCACAGG TTCAACCCCAGT	ATCGGGTACCTGAGCAGTG GATACACCTGAA
Screening Primer1	TGCTCCTGCCGAGAAAGTAT (Neo F)	CTATCAGGCCAACCTGTGGT (Gata1 R)
Screening Primer2	GAAGAGGCACTGGGAGTCAG (Gata1 F)	ATTCTCCCACCGTCAGTACG (CreERT2 R)
Guide RNA	**Sequence 5' to 3'**	
Non-Targeting-1	GTTCATTTCCAAGTCCGCTG	
Non-Targeting-3	GTATTACTGATATTGGTGGG	
Non-Targeting-4	TCATGCTTGCTTGGGCAAAA	
SgPU.1-2	GGGTACTGGAGGCACATCCG	
SgPU.1-3	AGACCTGGTGCCCTATGACA	
SgRUNX1-1	GGATGTTCCAGATGGCACTC	
SgRUNX1-2	GGTCATTAAATCTTGCAACC	

Supplemental Table 2. List of antibodies and the reagent suppliers used in these studies,

Human	**Fluorescence**	**Cat#**	**Vendor**
CD235a	APC	551336	BD Biosciences
CD71	FITC	334104	BioLegend
CD11b	PE	301305	BioLegend
Mouse	**Fluorescence**	**Cat#**	**Vendor**
CD71	FITC	113806	BioLegend
Ter119	APC	116212	BioLegend
CD44	APC-Cy7	103028	BioLegend
B220	FITC	103206	BioLegend
Gr1	FITC	108406	BioLegend
CD3e	FITC	100306	BioLegend
CD11b	FITC	101205	BioLegend
CD150	APC	115910	BioLegend
CD41	Alexa Fluor 700	133925	BioLegend
CD41	FITC	133904	BioLegend
CD61	APC	104315	BioLegend
FceRIa	FITC	134305	BioLegend
c-Kit	APC	105812	BioLegend
B220	Biotin	13-0452-85	ThermoFisher
CD2	Biotin	100103	BioLegend
CD3	Biotin	100304	BioLegend
CD5	Biotin	100604	Biolegend
CD8a	Biotin	100704	BioLegend
GR1	Biotin	13-5931-85	ThermoFisher
TER119	Biotin	116204	BioLegend
StAV	BV650	405232	BioLegend
c-Kit	APC-Cy7	105825	BioLegend
Sca1	BV421	108128	BioLegend
CD16/32	BV605	563006	BD Biosciences
CD105	PE-Cy7	120410	BioLegend
Sca1	APC	108111	BioLegend
CD16/32	PE-Cy7	101317	BioLegend
CD34	FITC	553733	BD Biosciences
Ter119	eF450	48-5921-82	ThermoFisher
Gr1	eF450	48-5931-80	ThermoFisher
B220	eF450	48-0452-82	ThermoFisher
CD3e	eF450	48-0032-82	ThermoFisher
CD11b	eF450	48-0112-80	ThermoFisher
CD41	eF450	48-0411-82	ThermoFisher
Live/Dead	**Fluorescence**	**Cat#**	**Vendor**
Annexin-V	PE	556421	BD Biosciences
DAPI	Pacific Blue	422801	BioLegend
Zombie Aqua	BV510	423101	Biolegend